Journal of Applied Sciences

ISSN 1812-5654

science alert

ANSInet
an open access publisher
http://ansinet.com

Journal of Applied Sciences 10 (3): 203-208, 2010
ISSN 1812-5654

Macro and Mesoscale Simulations of Free Convective Heat Transfer in a Cavity at Various Aspect Ratios

C.S.N. Azwadi and M.A.M. Irwan
Faculty of Mechanical Engineering, Universiti Teknologi Malaysia,
81310 UTM, Skudai, Johor, Malaysia

Abstract: In this study, we present the behavior of free convective heat transfer in a rectangular cavity by two entirely different scales of numerical methods, namely a mesoscale and macroscale methods. The cavity is bounded by two vertical isothermal walls kept at different temperatures and by two horizontal perfectly conducting walls. The heat flow simulations were carried out across the two isothermal walls by varying the aspect ratio of cavity with six different values -0.2, 0.5, 1.5, 2.0, 2.5 and 3.0. The macroscale simulations were performed by solving the Navier-Stokes equation using finite difference scheme while the mesoscale simulations were done using lattice Boltzmann method. This study found that the heat transfer mechanism, fluid flow behavior in terms of formation, size and strength of vortex are critically depending on the aspect ratio of the geometry. Numerical results also show excellent agreement between these two scales of simulations.

Key words: Aspect ratio, finite difference, lattice Boltzmann, natural convection, navier-stokes equation

INTRODUCTION

Free convective heat transfer is heat transfer between a surface and a fluid moving over it and the fluid motion is caused entirely by the buoyancy forces that arise due to the density changes which is initiated by temperature variations in the flow (Oosthuizen and Naylor, 1998). Since, the early works by various researchers, many theoretical and experimental researches were conducted to investigate this phenomenon on various condition such as flat surfaces (Clifton and Chapman, 1969; Hassan and Mohamed, 1970). The fundamental interest came from the concern to understand the heat transfer mechanism (Qi, 2008; Azwadi and Tanahashi, 2006; Laguerre *et al*., 2005) and fluid flow behavior around the surfaces (Ravnik *et al*., 2008; Yasin *et al*., 2009). Besides that, an identical interest was motivated by the wide range of engineering applications which involves this type of phenomenon (Kobus, 2005; Laguerre *et al*., 2009). In most of the problems related to free convection, many researchers focused their study on the heat transfer and fluid flow behavior from a differentially heated side walls in a cavity (Azwadi and Tanahashi, 2007; Lo *et al*., 2007). Most of the works were done by considering adiabatic boundary condition for the top and bottom walls. Only few investigated the effect of perfectly conducting top and bottom walls although it plays significant roles in real engineering applications (Oosthuizen and Naylor, 1998).

In this study, we carried out numerical investigation of natural convection in a square cavity by considering perfectly conducting boundary condition for top and bottom walls. The left and right walls were maintained at hot and cold temperature respectively. The aspect ratio (AR = height, H/width, W) is varied to six different values -0.2, 0.5, 1.5, 2.0, 2.5 and 3.0. Lattice Boltzmann simulation scheme is chosen as the mesoscale approach to see the dependence of mesoscale parameters on macroscale behavior. Lattice Boltzmann method derives the macroscopic equations from microscopic dynamics by means of statistics. Hence, it acts as a bridge between microscopic and macroscopic dynamics and therefore the method is considered to be a mesoscale method. For the macroscale simulation, we solve the Navier-Stokes directly and the finite difference scheme is brought as a discretization tool (Azwadi and Tanahashi, 2006).

It should be stated clearly that the objective of this study was not to make a comparison of both numerical algorithm with respect to computational efficiency, in terms of computational time or memory requirement. Therefore, besides the physics of the flow, the study focuses on the capability of the mesoscale method in simulating macroscale phenomenon.

PROBLEM PHYSICS AND BOUNDARY CONDITIONS

The physical domain of the problem is shown in Fig. 1. The temperature difference between the left and right walls creates a temperature gradient in the flow field, which will then introduce density difference. This

Corresponding Author: C.S. Nor Azwadi, Faculty of Mechanical Engineering, Universiti Teknologi Malaysia, 81310 UTM, Skudai, Johor, Malaysia

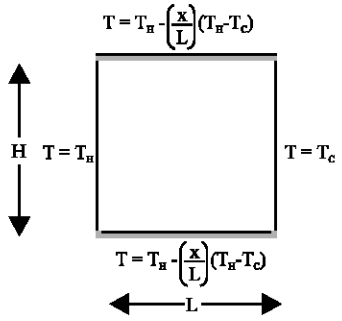

Fig. 1: Physical domain of the problem

Table 1: Computational mesh size for every aspect ratio

Mesh size	Aspect ratio
201×41	0.2
201×101	0.5
201×301	1.5
201×401	2.0
201×501	2.5
201×601	3.0

difference in density will cause the fluid to move. This movement is not initiated by any external force, therefore it is widely known as free convection. The top and bottom walls are assumed to be made from a material that has a relatively high thermal conductivity. Therefore, it is acceptable to assume that the temperature on these walls varies linearly with distance from hot left to cold right walls.

Boussinesq approximation is applied to the buoyancy force term. With this approximation, it is assumed that all fluid properties are constant except for density change with temperature.

$$G = \beta g(T-T_m)j \quad (1)$$

where, β is the thermal expansion coefficient, g is the acceleration due to gravity, j is the average temperature and T_m is the vertical direction opposite to that of gravity. The dynamical similarity depends on two dimensionless parameters: the Prandtl number Pr and Rayleigh number Ra:

$$Pr = v/x \quad (2)$$

$$R\alpha = \frac{\rho\beta(T_H - T_C)L^3}{vx} \quad (3)$$

where,v x and L are the fluid kinematic viscosity, thermal diffusivity and width of the cavity, respectively.

In all simulations, value of Pr and Ra are set at 0.71 and 10^5, respectively. The aspect ratio with the suitable mesh size is tabulated in Table 1.

MACROSCALE SIMULATION

For macroscale simulation, the governing equation is the incompressible, two-dimensional and laminar Navier-Stokes equation and the energy equation. These governing equations were solved directly using stream function vorticity finite difference formulation. To begin, the equations can be written as follows:

$$\frac{\partial u}{\partial x} + \frac{\partial v}{\partial y} = 0 \quad (4)$$

$$u\frac{\partial u}{\partial x} + v\frac{\partial v}{\partial y} = -\frac{1}{\rho}\frac{\partial p}{\partial x} + v\left(\frac{\partial^2 u}{\partial x^2} + \frac{\partial^2 v}{\partial y^2}\right) \quad (5)$$

$$u\frac{\partial u}{\partial x} + v\frac{\partial v}{\partial y} = -\frac{1}{\rho}\frac{\partial p}{\partial x} + v\left(\frac{\partial^2 u}{\partial x^2} + \frac{\partial^2 v}{\partial y^2}\right) + \beta g(T - T_1) \quad (6)$$

$$u\frac{\partial T}{\partial x} + v\frac{\partial T}{\partial y} = \left(\frac{k}{\rho c_p}\right)\left(\frac{\partial^2 T}{\partial x^2} + \frac{\partial^2 T}{\partial y^2}\right) \quad (7)$$

The pressure terms are eliminated by taking the y-derivative of Eq. 6 and subtracting from it the x-derivative of Eq. 5. This gives:

$$u\left(\frac{\partial^2 v}{\partial x^2} - \frac{\partial^2 u}{\partial x\partial y}\right) + v\left(\frac{\partial^2 v}{\partial y\partial x^2} - \frac{\partial^2 u}{\partial y^2}\right) + \frac{\partial u}{\partial x}\left(\frac{\partial u}{\partial x} + \frac{\partial v}{\partial y}\right) - \frac{\partial u}{\partial y}\left(\frac{\partial u}{\partial x} + \frac{\partial v}{\partial y}\right) = v\left[\left(\frac{\partial^3 v}{\partial x^3} - \frac{\partial^3 v}{\partial x^2\partial y}\right) + \left(\frac{\partial^3 v}{\partial y^2\partial x} - \frac{\partial^3 u}{\partial y^3}\right)\right] - \beta g\frac{\partial t}{\partial x} \quad (8)$$

Using the definition of vorticity and continuity Eq. 8 can be written as:

$$u\frac{\partial \omega}{\partial x} + v\frac{\partial \omega}{\partial x} = v\left(\frac{\partial^2 \omega}{\partial x^2} + \frac{\partial^2 \omega}{\partial y^2}\right) - \beta g\left(\frac{\partial t}{\partial x}\right) \quad (9)$$

In terms of the stream function, this equation becomes:

$$\frac{\partial \Psi}{\partial y}\frac{\partial \omega}{\partial x} - \frac{\partial \Psi}{\partial x}\frac{\partial \omega}{\partial y} = v\left(\frac{\partial^2 \omega}{\partial x^2} + \frac{\partial^2 \omega}{\partial y^2}\right) - \beta g\left(\frac{\partial t}{\partial x}\right) \quad (10)$$

In terms of the stream function, the equation defining the vorticity becomes:

$$\left(\frac{\partial^2 \Psi}{\partial x^2} + \frac{\partial^2 \Psi}{\partial y^2}\right) = -\omega \quad (11)$$

while in terms of the stream function, the energy equation becomes:

$$\frac{\partial \psi}{\partial y}\frac{\partial T}{\partial x}-\frac{\partial \psi}{\partial x}\frac{\partial T}{\partial y}=\left(\frac{k}{\rho c_p}\right)\left(\frac{\partial^2 T}{\partial x^2}+\frac{\partial^2 T}{\partial y^2}\right) \quad (12)$$

Before considering the numerical solution to the above set of equations, the equations need to be rewritten in terms of dimensionless variables. The following dimensionless variables were used:

$$\Psi=\frac{\psi Pr}{v},\ \Omega=\frac{\omega L^2 Pr}{v}$$

$$X=\frac{x}{L},\ Y=\frac{y}{L},\ \theta=\frac{T-T_c}{T_H-T_c} \quad (13)$$

In terms of these variables, Eq. 10-12 becomes:

$$\frac{\partial^2 \Omega}{\partial X^2}+\frac{\partial^2 \Omega}{\partial Y^2}=\frac{1}{Pr}\left(\frac{\partial \Psi}{\partial Y}\frac{\partial \Omega}{\partial X}-\frac{\partial \Psi}{\partial X}\frac{\partial \Omega}{\partial Y}\right)+Ra\frac{\partial \theta}{\partial X} \quad (14)$$

$$\left(\frac{\partial^2 \Psi}{\partial X^2}+\frac{\partial^2 \Psi}{\partial Y^2}\right)=-\Omega \quad (15)$$

$$\left(\frac{\partial^2 \theta}{\partial X^2}+\frac{\partial^2 \theta}{\partial Y^2}\right)=\frac{\partial \Psi}{\partial Y}\frac{\partial \theta}{\partial X}-\frac{\partial \Psi}{\partial X}\frac{\partial \theta}{\partial Y} \quad (16)$$

Finally, Eq. 14-16 are solved using an iterative, uniform mesh finite difference solution procedure with second order accuracy.

MESOSCALE SIMULATION

As an alternative approach, the governing equations are solved indirectly using lattice Boltzmann method. The main difference between lattice Boltzmann method and other numerical methods is that it predicts the evolution of particles displacement due to collision and streaming in mesoscale point of view which is represented by a distribution function. This distribution function can then be used to calculate the macroscopic variables by taking moment to the distribution function. Therefore, lattice Boltzmann method links mesoscale variables with macroscale variables similar to the previous discussed method.

The Boltzmann equation, discretized in space and time, is given as follows:

$$f_i(x+c_i\Delta t,t+\Delta t)-f_i(x,t)=-\frac{1}{\tau_f}\left(f_i-f_i^{eq}\right)+1 \quad (17)$$

$$g_i(x+c_i\Delta t,t+\Delta t)-g_i(x,t)=-\frac{1}{\tau_g}\left(g_i-g_i^{eq}\right) \quad (18)$$

where, distribution function f is used to calculate density and velocity fields and distribution function g is used to calculate temperature field. F is the external force and τ_f and τ_g are the relaxation times carried by the momentum and energy, respectively.

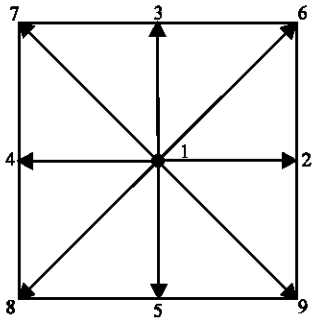

Fig. 2: Nine-velocity lattice model with w_1 = 4/9, $w_{2,3,4,5}$ = 1/9 and $w_{6,7,8,9}$ = 1/36

The equilibrium distribution functions f_i^{eq} and g_i^{eq} are defined so that they satisfy the macroscopic Eq. 4-7 through the Chapman-Enskog expansion. They can be expressed as follow (Azwadi and Tanahashi, 2008):

$$f_i^{eq}=w_i\rho\left[1+3c_i\cdot u+4.5(c_i\cdot u)^2-1.5u^2\right] \quad (19)$$

$$g_i^{eq}=w_i\rho\left[1+3c_i\cdot u+4.5(c_i\cdot u)^2-1.5u^2\right] \quad (20)$$

The values of the weight w_i is decided according to the chosen lattice model. In this study, we choose a nine-velocity lattice model to represent both the f and g distribution functions. The lattice configuration is shown in Fig. 2.

The macroscopic variables such as density, velocity and temperature can be calculated by taking moment to the distribution functions as follows:

$$\rho=\sum_1^9 f_i,\ \rho u=\sum_1^9 c_i f_i,\ \rho T=\sum_1^9 c_i g_i \quad (21)$$

The time relaxations can be related to the macroscopic fluid kinematic viscosity and thermal diffusivity using the following equations:

$$\tau_f=3v+\frac{1}{2} \quad (22)$$

$$\tau_g=3\chi+\frac{1}{2} \quad (23)$$

RESULTS AND DISCUSSION

Figure 3a, b and 4a, b show the plots of streamline and isothermal line obtained by mesocale and macroscale numerical methods for Rayleigh number of 10^5 and Prandtl number of 0.71. In present study, we solve the discretised

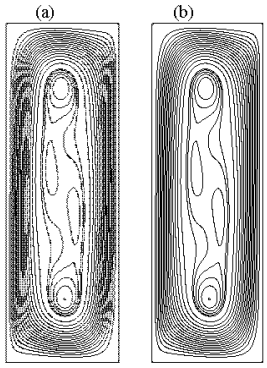

Fig. 3: Streamline plots by (a) macroscale and (b) mesoscale simulation at AR = 3.0

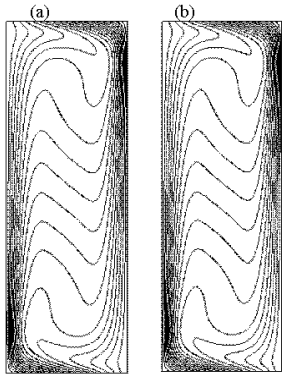

Fig. 4: Isothermal line plots by (a) macroscale and (b) mesoscale simulation at AR = 3.0

the equations using FORTRAN developed in this study. As can be seen from the Fig. 3 and 4, it is obvious that macroscale and mesoscale simulation results are identical. Comparisons also have been carried out for other aspect ratios -0.2, 0.5, 1.5, 2.0 and 2.5 at the same values of Rayleigh and Prandtl numbers and excellent quantitative agreements were found (not shown).

For the purpose of results interpretation, we brought the results obtained from macroscale computation and shown in Fig. 5-7. For aspect ratio less than 1.0 shown in Fig. 5a and b, a unicellular circulating flow pattern is observed which creates unicellular convection roll. The streamlines form a single vortex with its center at the center of the system. As the aspect ratio is increased, the vortex that was horizontally elliptic evolves into a less elliptic shape resembling a circle. At this low aspect ratio, the perfectly conducting walls are relatively closer, while the isothermal walls are far apart.

For aspect ratio greater than 1.0 (Fig. 6a-d), the hot and cold walls get closer. The central streamline elongates

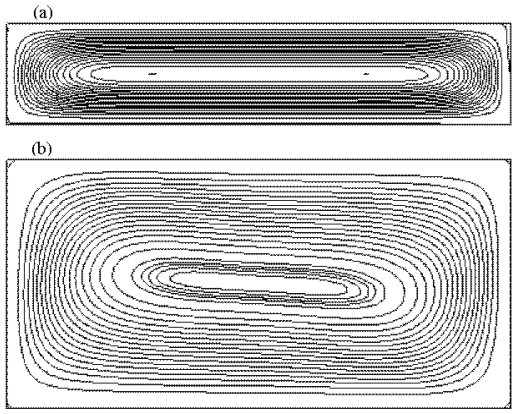

Fig. 5: Streamline plots for AR<1.0 by macroscale simulation, (a) AR = 0.2 and (b) AR = 0.5

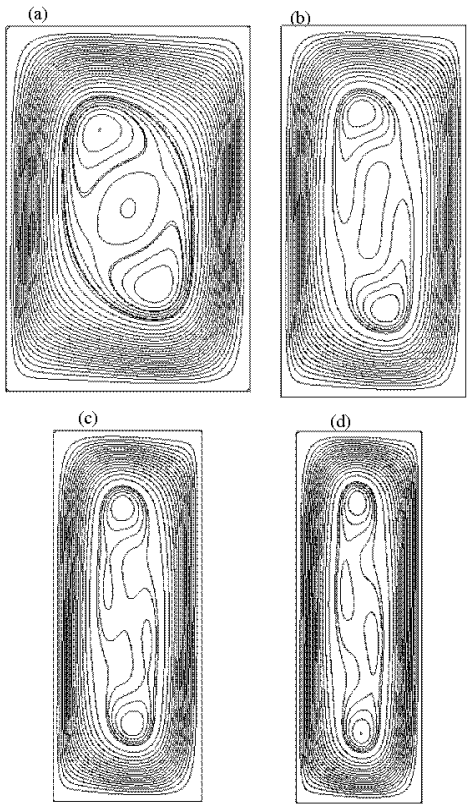

Fig. 6: Streamline plots for AR > 1.0 by macroscale simulation, (a) AR = 1.5, (b) AR = 2.0, (c) AR = 2.5 and (d) AR = 3.0

and additional vortices start to develop inside it. When the aspect ratio is further increased, the central streamline elongates to form elliptic shape again but vertically. The

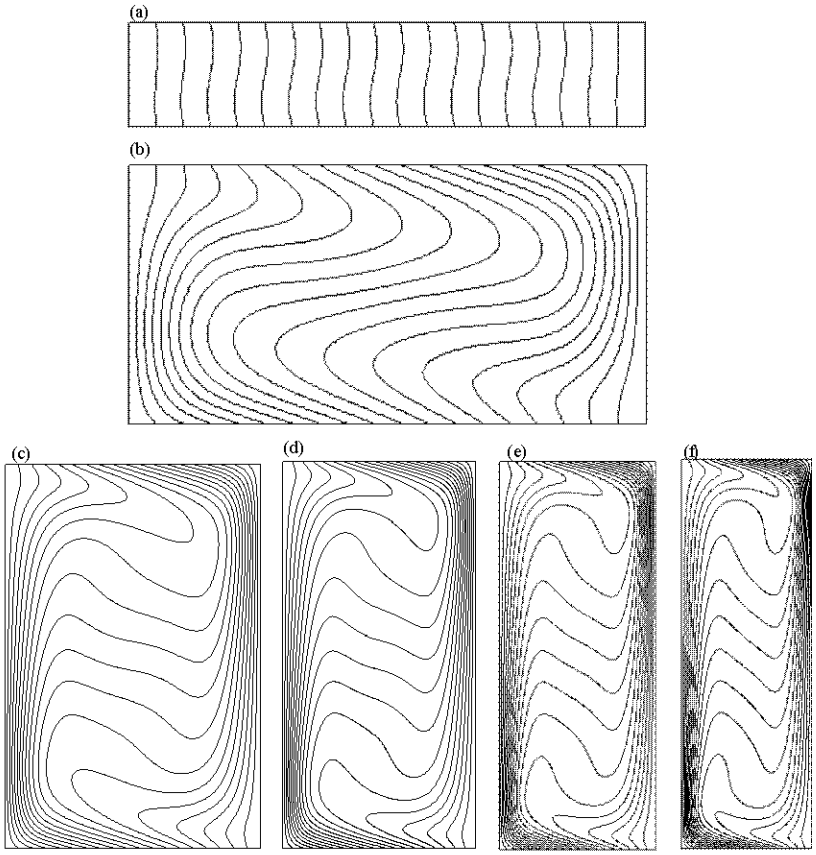

Fig. 7: Isothermal line plots by macroscale simulation, (a) AR = 0.2, (b) AR = 0.5, (c) AR = 1.5, (d) AR = 2.0, (e) AR = 2.5 and (f) AR = 3.0

vortices become smaller and new vortices develop within the earlier vortices (formation of single convective rolls). These phenomena agree well with previous studies (Rahman and Shariff, 2005).

Figure 7a-f demonstrate the isothermal lines for aspect ratio ranged from 0.2 to 3.0. At aspect ratio (AR = 0.2), the lines are vertical and parallel to the heated walls which indicates that the dominant heat transfer mode is by conduction. For higher aspect ratios, the vertical lines start to distort from left wall to right wall for the upper part and distort from right wall to left wall for the lower part. This shows that as the aspect ratio increases, conduction heat transfer becomes less significant and convection heat transfer dominates due to smaller gap between the hot and cold walls and convection mode becomes stronger. However, it can be observed that the vertical lines near the hot and cold walls are denser compared to other regions in the system. In this region, conduction heat transfer still dominates the heat transfer mechanism.

CONCLUSION

The present study was conducted due to lack of accurate and detailed data found in the literature for the natural convection in differentially heated side walls and perfectly conduction top and bottom walls. In order to generate reliable numerical results, two totally different numerical scales were applied to investigate the fluid flow behaviour and heat transfer mechanism in the confined system for Rayleigh number at 10^5, Prandtl number 0.71 and aspect ratio range 0.2 to 3.0. Both numerical methods applied second order accuracy for space and time. The flow pattern for every simulation condition was evaluated in terms of streamline plots, the deviation between the mesoscale of lattice Boltzmann method and macroscale of finite different Navier-Stokes method are almost negligible. Finally the heat transfer mechanism in the system were computed and compared. Convection effect increases as the aspect ratio increases, implying that the convective flow inside the cavity becomes more vigorous

as the enclosure shape changes from low to high aspect ratio and good agreement with the results in the literature. The results obtained are evidence that mesoscale simulation can be used as an alternative approach to solve macroscale simulation. The extension to 3D computations and higher Rayleigh numbers is the subject of further investigations within ongoing research.

ACKNOWLEDGMENTS

The authors would like to thank Universiti Teknologi Malaysia (UTM) and the Malaysia government for supporting this study.

REFERENCES

Azwadi, C.S.N. and T. Tanahashi, 2006. Simplified thermal lattice Boltzmann in incompressible limit. Int. J. Mod. Phys. B., 20: 2437-2449.

Azwadi, C.S.N. and T. Tanahashi, 2007. Three-dimensional thermal lattice Boltzmann simulation of natural convection in a cubic cavity. Int. J. Mod. Phys. B., 21: 87-96.

Azwadi, C.S.N. and T. Tanahashi, 2008. Simplified finite difference thermal lattice Boltzmann method. Int. J. Mod. Phys. B., 22: 3865-3876.

Clifton, J.V. and A.J. Chapman, 1969. Natural convection on a finite-size horizontal plate. Int. J. Heat Mass Transfer, 12: 1573-1584.

Hassan, K.E. and S.A. Mohamed, 1970. Natural convection from isothermal flat surfaces. Int. J. Heat Mass Transfer, 13: 1873-1886.

Kobus, C.J., 2005. Utilizing disk thermistors to indirectly measure convective heat transfer coefficients for forced, natural and combined (mixed) convection. Exp. Thermal Fluid Sci., 29: 659-669.

Laguerre, O., D. Remy and D. Flick, 2009. Airflow, heat and moisture transfers by natural convection in a refrigerating cavity. J. Food Eng., 91: 197-210.

Laguerre, O., S.B. Amara and D. Flick, 2005. Experimental study of heat transfer by natural convection in a closed cavity: Application in a domestic refrigerator. J. Food Eng., 70: 523-537.

Lo, D.C., D.L. Young and C.C. Tsai, 2007. High resolution of 2D natural convection in a cavity by the DQ method. J. Comput. Appl. Math., 203: 219-236.

Oosthuizen, P.H. and D. Naylor, 1998. Introduction to Convective Heat Transfer Analysis. Int. Edn., McGraw-Hill, Singapore.

Qi, H.D., 2008. Fluid flow and heat transfer characteristics of natural convection in a square cavities due to discrete source-sink pairs. Int. J. Heat Mass Transfer, 51: 5949-5957.

Rahman, M. and M.A.R. Sharif, 2005. Numerical study of laminar natural convection in inclined rectangular enclosures of various aspect ratios. Numerical Heat Transfer Part A: Appl., 48: 355-373.

Ravnik, J., L. Skerget and Z. Zunic, 2008. Velocity-vorticity formulation for 3D natural convection in an inclined enclosure by BEM. Int. J. Heat Mass Transfer, 51: 4517-4527.

Yasin, V., F.O. Hakan, K. Ahmet and O. Filiz, 2009. Natural convection and fluid flow in inclined enclosure with a corner heater. Appl. Thermal Eng., 29: 340-350.